CHEMISTRY
A EUROPEAN JOURNAL

DOI: 10.1002/chem.200800593

Belizeanic Acid: A Potent Protein Phosphatase 1 Inhibitor Belonging to the Okadaic Acid Class, with an Unusual Skeleton

Patricia G. Cruz,[a] José Javier Fernández,*[a] Manuel Norte,*[a] and Antonio Hernández Daranas*[a, b]

Abstract: Belizeanic acid (BA), a novel metabolite belonging to the okadaic acid class of protein phosphatase inhibitors, was isolated from artificial cultures of the dinoflagellate *Prorocentrum belizeanum*. The structure and conformational behaviour of BA was elucidated by a combination of NMR spectroscopy and conformational analysis. The isolation of this metabolite, which possesses a simplified version of the okadaic acid skeleton, supports the biogenetic pathway previously reported for this class of compounds. BA showed potent inhibitory activity against protein phosphatase 1 (PP1) within the nM range. A plausible model for the interaction of BA with the PP1 binding pocket was derived from computational docking studies.

Keywords: biosynthesis · conformation analysis · enzyme inhibitors · natural products · structure elucidation

Introduction

Okadaic acid (OA), a toxic polyether produced by dinoflagellates of the genera *Prorocentrum* and *Dinophysis*,[1,2] is the main agent responsible for diarrethic shellfish poisoning (DSP) syndrome.[3] Due to its significance for public health and the economy of the fishing industry, many programmes have been implemented to monitor and control these toxins.[4] Therefore, it is important to increase the number of targets for the chemical analysis of contaminated shellfish.

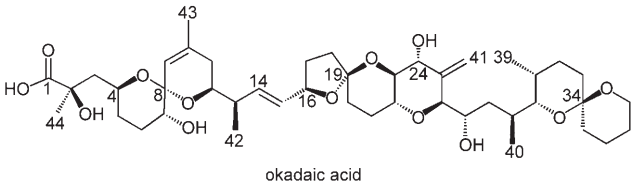

okadaic acid

OA is also a well-known tumour promoter.[5] This fact has been decisive in unlocking the secret of its mechanism of action, which involves selective inhibition of serine/threonine protein phosphatases (PPs).[6,7] Thus, OA is now recognised as the first member of the okadaic acid class of PP inhibitors, an unusual group of metabolites that have become valuable tools for studying the cellular roles of different PPs.[8] As a result of their use, the essential role of PPs in the regulation of processes such as metabolism, signal transduction and the control of cell growth and death has been accepted. Nowadays, PP inhibitors are used in studies directed towards understanding diseases such as cancer, Alzheimer's and diabetes. Not surprisingly, these findings have prompted a number of laboratories to pursue the total synthesis of okadaic acid.[9–11] Thus, structural studies of PP1 and PP2A in parallel with the search for new inhibitors and an understanding of their conformational properties in solution has the potential to provide valuable insights into their binding processes.

Here we report on the isolation, structure determination and inhibitory activity of a new *Prorocentrun belizeanum*

[a] Dr. P. G. Cruz, Prof. J. J. Fernández, Prof. M. Norte, Dr. A. H. Daranas
Instituto Universitario de Bio-Orgánica "Antonio González"
Universidad de La Laguna
Av. Astrofísico Francisco Sánchez 2. 38206
La Laguna, Tenerife (Spain)
Fax: (+34) 922-318571
E-mail: jjfercas@ull.es
mnorte@ull.es
adaranas@ull.es

[b] Dr. A. H. Daranas
Departamento de Ingeniería Química y
Tecnología Farmacéutica, Universidad de La Laguna
Av. Astrofísico Francisco Sánchez s/n. 38071
La Laguna, Tenerife (Spain)
Fax: (+34) 922318004

Supporting information for this article is available on the WWW under http://dx.doi.org/10.1002/chem.200800593.

toxin, belizeanic acid (BA). Although this compound did not possess the characteristic carbon skeleton of OA, it shares enough structural elements to be considered an OA analogue. Moreover, the new structure gives important clues about the biosynthetic origin of these molecules.

Results and Discussion

Cultures and isolation: Large-scale cultures of the microalgae *P. belizeanum* were carried out statically in 80-L tanks at 21 °C, using Guillard K medium under a 16:8 light/dark cycle up to a final volume of 1020 L. After 45 days, cells were harvested by centrifugation at $3500 \times g$ and the resultant pellet was sonicated at room temperature with acetone affording, after solvent evaporation in vacuo, a brown extract (21 g). The crude extract was subsequently fractionated by gel filtration chromatography (Sephadex LH-20), eluting with a mixture of $CHCl_3$/MeOH/*n*-hexane (1:1:2). The active fraction was subjected to further reverse-phase chromatography (Lobar RP-18), eluting with MeOH/H_2O (17:3). Finally, BA was purified by preparative reverse-phase HPLC using an XTerra column with CH_3CN/H_2O (7:3) as mobile phase.

Structural determination: BA was isolated as a white amorphous solid, with $[\alpha]_D^{25} = +2.7$. Analysis of its mass spectra revealed a molecular formula of $C_{44}H_{72}O_{14}$ (*m*/*z*: 847.4820 $[C_{44}H_{72}O_{14}Na]^+$), and its IR spectrum showed an intense band at 1732 cm^{-1}, characteristic of a carboxyl group.

Comparison of the ^1H NMR spectra of BA with that shown by okadaic acid revealed chemical-shift differences around the C-11→C-24 fragment (Table 1).[12] However, fragments C-3→C-7, C-26→C-33 and C-35→C-38, which were established through COSY connectivities, turned out to be identical to those observed in OA. Analysis of HSQC and HMBC spectra indicated the presence of six quaternary, 17 methine, 16 methylene and five methyl carbons. On the basis of these carbon chemical shifts it was concluded that BA is composed of one carboxyl group and three double bonds that accounted for four of the total nine degrees of unsaturation implied by the molecular formula, indicating that BA contained five rings. Thus, C-3 was connected to C-2 through HMBC cross peaks between C-2 ($\delta_C = 76.6$) and C-3 ($\delta_C = 46.2$) with H_3-44 ($\delta_H = 1.20$), and the carboxylic carbon C-1 was joined from the correlations of C-1 ($\delta_C = 182.5$) with H-3 ($\delta_H = 1.60$) and H_3-44 ($\delta_H = 1.20$) (Figure 1).

Table 1. ^1H and ^{13}C NMR chemical-shift differences observed in CD_3OD for okadaic acid versus belizeanic acid.

	Okadaic acid		Belizeanic acid	
Carbon	δ ^{13}C	δ ^1H	δ ^{13}C	δ ^1H
15	131.9	5.34	133.9	5.44
16	80.2	4.52	71.9	3.97
17	31.0	2.08/1.43	31.8	1.65 (2H)
18	37.7	1.88/1.72	31.0	1.52 (2H)
19	106.5	–	70.7	3.57
20	33.4	1.84/1.72	27.6	1.60 (2H)
21	27.5	1.90/1.75	27.3	2.08 (2H)
22	71.1	3.50	74.0	3.55
23	78.1	3.28	78.1	2.91
24	71.8	3.92	73.8	3.93

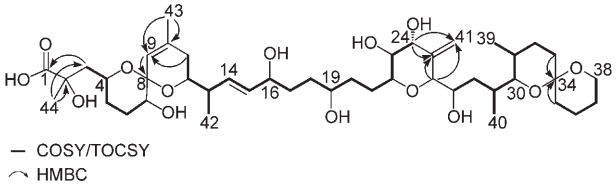

Figure 1. NMR-derived correlations observed for belizeanic acid. COSY and TOCSY connectivities (represented by bold lines) defined four partial structures separated by quaternary carbons that were connected through HMBC (indicated by arrows).

In the same way, the fragment C-8→C-11 including the quaternary carbons C-8 and C-10 was established on the basis of HMBC correlations between H-9 ($\delta_H = 5.18$) with C-8 ($\delta_C = 97.6$), C-11 ($\delta_C = 33.6$) and C-43 ($\delta_C = 22.5$), as well as H_3-43 ($\delta_H = 1.65$) with C-10 ($\delta_C = 139.3$). Finally, fragments C-26→C-33 and C-35→C-38 were joined on the basis of the cross peaks observed in the HMBC for C-34 ($\delta_C = 96.2$) with H_2-33 ($\delta_H = 1.27$) and H-35 ($\delta_H = 1.54$).

The elucidation of the largest spin system C-11→C-24 was defined using selective 1D TOCSY, as well as 2D COSY, HSQC and HMBC. Analysis of the HSQC and HMBC spectra confirmed the presence in this fragment of two olefinic methines, six oxymethines, one allylic methine, five methylenes and one methyl group. Therefore, the most evident difference to OA was the absence of the characteristic acetalic carbon C-19 and the presence of a new oxymethine ($\delta_C = 70.7$). The correlation process started from the double bond C-14→C-15 in the following sequence: H-14 ($\delta_H = 5.74$) was first correlated to H-15 ($\delta_H = 5.44$) and H-13 ($\delta_H = 2.26$). Later, H-13 connected to H-12 ($\delta_H = 3.72$) and H_3-42 ($\delta_H = 1.03$) and H-12 subsequently to both H_2-11 ($\delta_H = 1.91$ and 1.73). In the same manner, H-15 was correlated to H-16 ($\delta_H = 3.97$) and this in turn to both H_2-17 ($\delta_H = 1.65$). At this point, due to signal overlap, the correlation between the methylenes H_2-17 and H_2-18 ($\delta_H = 1.52$) was established using selective 1D TOCSY. Analysis of this fragment was completed using the COSY spectrum, which showed the following correlations: H_2-18 ($\delta_H = 1.52$)→H-19 ($\delta_H = 3.57$)→H_2-20 ($\delta_H = 1.60$)→H_2-21 ($\delta_H = 2.08$)→H-22 ($\delta_H = 3.55$)→H-23 ($\delta_H = 2.91$)→H-24 ($\delta_H = 3.93$). In contrast to OA, the C-11→C-24 fragment accounts for the two extra unsaturations present in BA, as two rings out of the tricyclic system characteristic of OA are now open in BA. In addition, the proposed structure explains the absence of the acetalic carbon C-19 and the presence of three carbons bearing hydroxyl groups: C-16 ($\delta_C = 71.9$), C-19 ($\delta_C = 70.7$) and C-23 ($\delta_C = 78.1$), thus accounting for the extra oxygen atom present in BA. Finally, the connection of the C-11→C-24 fragment to the rest of the molecule was shown using the HMBC spec-

trum. In this way, C-25 ($\delta_C = 146.4$) was correlated with both H-24 ($\delta_H = 3.93$) and H-26 ($\delta_H = 3.82$), and both H_2-41 ($\delta_H =$ 5.18 and 4.92) correlated with C-24 ($\delta_C = 73.8$) and C-26 ($\delta_C = 85.1$).

The relative configuration of most chiral centres in BA (Figure 2) were determined by a combination of *J*-based configurational analyses and dipolar correlations as observed in the ROESY spectrum, comparing the results with those characteristic of OA. The data obtained for the C-1→C-15 and C-26→C-38 regions in BA turned out to be equivalent to those typical for OA. Thus, H-4 ($\delta_H = 3.97$) showed ROE cross-correlation peaks with H-5α ($\delta_H = 1.20$), H-6α ($\delta_H = 1.83$) and H-12 ($\delta_H = 3.72$), whereas H-7 ($\delta_H = 3.27$) connected with H-5β ($\delta_H = 1.70$) and H-9 ($\delta_H = 5.18$). In the same way, H-12 ($\delta_H = 3.72$) showed connectivities with H-14 ($\delta_H = 5.74$) and H_3-42 ($\delta_H = 1.03$) and the usual correlations between H-15 ($\delta_H = 5.44$) and H-13 ($\delta_H = 2.26$) and H-16 ($\delta_H = 3.97$) were also defined. These data together with the measured coupling constants allowed us to determine relative stereochemistries at C-4, C-7, C-8, C-12 and C-13 as identical to those of OA. The configuration of the double bond C-14=C-15 was determined as *E* on the basis of the large value of $^3J_{H14,H15} = 15.5$ Hz (Figure 2).

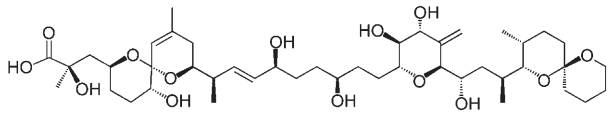

Figure 2. Structure of belizeanic acid with the proposed relative stereochemistry.

Relative configurations of C-22, C-23, C-24 and C-26 were established by analysis of the coupling constants $J_{H22,H23} = 9.8$ and $J_{H23,H24} = 7.1$ Hz together with the ROE correlations between H-22 ($\delta_H = 3.55$) and H-24 ($\delta_H = 3.93$). In the same way, ROE correlations of H-26 ($\delta_H = 3.82$) with H-41 ($\delta_H = 4.92$) and H-28 ($\delta_H = 1.29$), as well as between H-27 ($\delta_H = 3.98$) and H-28′ ($\delta_H = 0.85$) and H_3-40 ($\delta_H = 0.97$), in combination with characteristic anti-coupling constants $J_{H26,H27} = 8.8$, $J_{H27,H28(1.29)} = 9.2$, $J_{H28'(0.85),H29} = 9.4$ and $J_{H29,H30} =$ 9.8 Hz, indicated a relative stereochemistry of carbons C-26, C-27, C-29 and C-30 as identical to OA.

Likewise, relative stereochemistries for the chiral centres at the C-30→C-38 region were determined based on the key ROE correlations of H-31 ($\delta_H = 1.74$) with H-29 ($\delta_H = 1.82$) and H_3-39 ($\delta_H = 0.85$), whereas the chirality at C-34 was determined by correlations of H-38β ($\delta_H = 3.63$) with H-30 ($\delta_H = 3.18$) and H_3-40 ($\delta_H = 0.97$).

However, the chirality of the stereocentres located in the long acyclic part of BA, at C-16 and C-19, could not be assigned on the basis of the previous analysis. A possible solution for this problem is based on the results of a molecular-mechanics approach to determine the relative configuration of these chiral centres in combination with NMR data.[13–15]

Conformational study: Once the planar structure and the stereochemistry of most chiral centres of BA were determined, a conformational study was carried out in order to determine the configuration of carbons C-16 and C-19. We decided to study the four possible isomers 16*S**19*S**, 16*S**19*R**, 16*R**19*S** and 16*R**19*R**, and for this, extensive Monte Carlo multiple minimum (MCMM) conformational searches (100 000 steps) and molecular dynamics (MD) were undertaken for each of the four possible stereoisomeric structures of BA.

The crystal structure of OA was used as a template to build the structure of BA by removal of the appropriate covalent bonds.[16] The chirality of C-16 and C-19 was then adapted to build the four possible diastereoisomers and the resulting structures were used as the starting point for the conformational searches. Based on previous results obtained in our laboratory with these kinds of molecules,[17,18] these consisted of four independent searches with the MMFF94s[19] force field as implemented in MacroModel 8.5[20] using the generalised Born/surface area (GBSA) water-solvent model.[21] Random searches of 100 000 MCMM steps were undertaken for each diastereoisomer to ensure that the potential energy surface was thoroughly explored using the TNCG algorithm. All local minima within 50 kJ of the global minimum were saved and subsequently re-minimised using the FMNR algorithm and an energy cutoff of 25 kJ to save the resulting molecules. Afterwards, a search within each conformer pool was performed to select only those structures showing *anti* conformations of the C-26→C-30 region as deduced by the measured $^3J_{H,H}$ values (only those structures having dihedral angles within a range of 180 ± 40° were selected). The previous filtering step was followed by a combination of all the selected structures obtained from each conformer pool (this is from each stereoisomer), the subsequent adaptation of the chirality (16*S**19*S**, 16*S**19*R**, 16*R**19*S**, 16*R**19*R**) to yield four pools containing the "same" conformers and a multiple minimisation for each diasteroisomer using the FMNR algorithm saving those conformers within an energy cutoff of 25 kJ of the global minimum for each search.

As a representative example of the four possible stereoisomers of BA, for the 16*S**19*S** the previous procedure generated 486 structures for the conformational pool. Afterwards, XCluster[22] was employed to group conformations into a more manageable set of structurally related classes. Finally, by visual examination of the 48 conformers obtained from the previous step, we identified eight representative structural motifs (Figure 3). In this way, even though superposition of members of a given class does not result in perfectly aligned ensembles, they show the preferred arrangements in conformational space.

Compared to the crystallographic structure of OA,[16] the global minimum found for 16*S**19*S** BA shows individually superimposable substructures in the C-1→C-16 and C-21→C-38 fragments. However, the aperture of the ring system C-16→C-22 characteristic of OA confers BA a higher flexibility and the result according to our calculations is a mole-

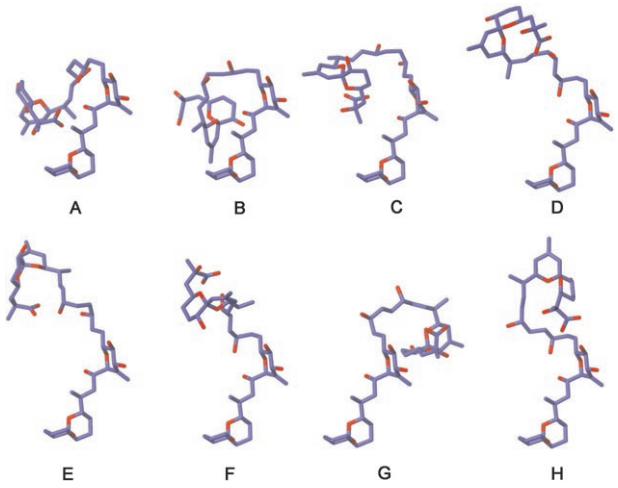

Figure 3. Comparison of the eight different structural motifs obtained from the MCMM conformational search conducted for the 16*S**19*S** stereoisomer of belizeanic acid.

cule that shows a turn in the opposite direction to that of OA (Figure 4). The same is true for nearly all the other families in which the differences are mostly in the torsion angles

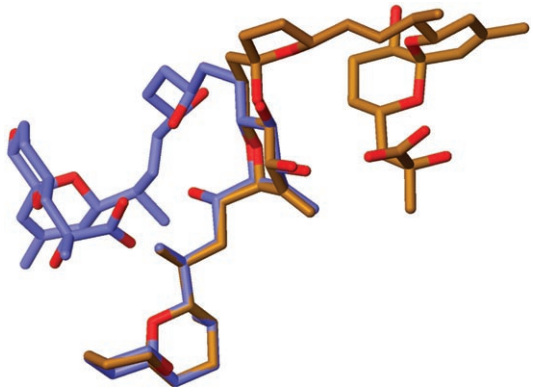

Figure 4. Crystal structure of okadaic acid (gold) overlapped (using the C30–C38 ring system) with lowest-energy conformer found for the 16*S**19*S** stereoisomer of beliezeanic acid (blue).

around the C-17→C-21 region, the less-populated families (labeled G and H in Figure 3) being the two exceptions in which the left-hand turn characteristic of OA is also present, though with some differences. Notably, for the 16*S**19*S** isomer the global minimum found shows a favorable energetic difference of 9 kJ mol^{-1} relative to the top structure of the second best conformational family (see Supporting Information). Similar results were obtained for the analysis performed with the other diastereoisomers of BA.

To analyze conformational equilibrium in BA further, four MD simulations of 4 ns (one for each possible diasteroisomer) starting from the global minimum found in each conformational search were performed using the MMFF94s force field and the GBSA water-solvent model as implemented in Macromodel 8.5.[17–19] The results of these simulations agree with those obtained from the conformational searches. Even though BA is a flexible molecule, it seems that it adopts preferred conformations in solution, the most populated ones being those showing the lowest energies in the MCMM searches. Note that the resulting ensemble-averaged (derived from the estimated populations by a Boltzmann distribution at 300 K) structures obtained for each diasteroisomer from the MCMM searches and the time-averaged ones obtained from the MD trajectories matched very well (Figure 5).

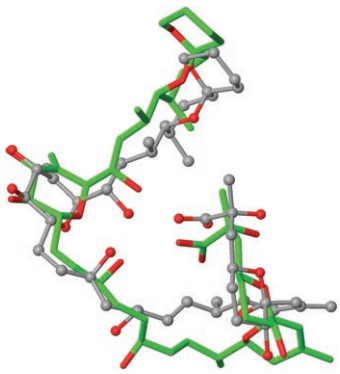

Figure 5. Superposition of the MCMM (grey) and MD (yellow) averaged structures for the 16*S**19*S** stereoisomer of belizeanic acid.

Therefore, the data obtained from the MD simulations were compared to the NMR data available for BA. The results of such comparisons were that only the time-averaged structure of the 16*S**19*S** diasteroisomer matched appropriately with the experimental NMR data. The key data used to discard the three other possibilities were the H-14–H-16 distance of 2.55 Å as obtained from the ROESY data, as well as the $^{3}J_{H15,H16}=7.0$ Hz attributable to an *anti* conformation. As can be observed from Figure 6, only the 16*S**19*S** diastereoisomer shows a relatively stable distance of around 2.5 Å that matches very well with the distance deduced from the ROESY experiment. At the same time, only the 16*S**19*S** isomer maintains the H-15-C-15-C-16-H-16 dihedral angle constant around an *anti* conformation (average value of 170°), as opposed to the other diasteroisomers that show *gauche* conformations most of the time. Consequently, we propose the 16*S**19*S** stereochemistry as the most plausible for BA.

Biosynthetic hypothesis: Different research groups have studied the biosynthetic origin of OA[23,24] and have found it to be a typical example of a nonclassic polyketide. In one of these studies, Murata et al. determined the biosynthetic origin of the oxygen atoms present in OA by using ^{18}O labelled precursors and MS spectrometry.[25,26] They concluded that most oxygen atoms in OA derive from atmospheric oxygen, the only exceptions being the hydroxyls located at C-8, C-27 and the oxygen at the tetrahydrofuranic ring in

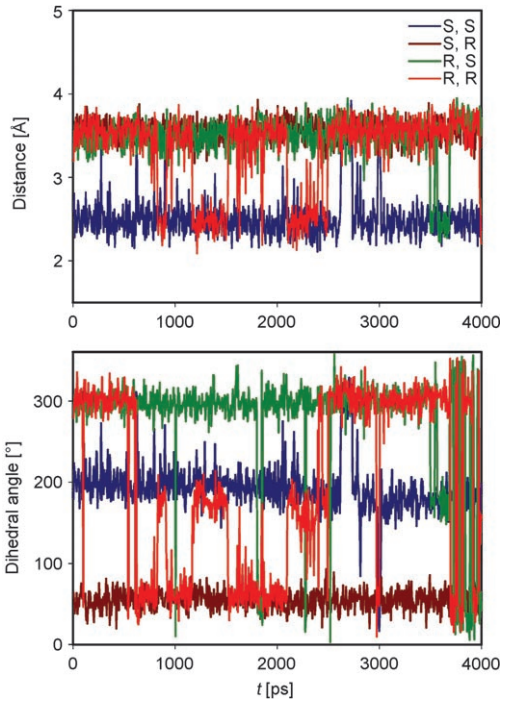

Figure 6. MD trajectories showing the evolution of the H-14–H-16 distance and the H-15-C-15-C-16-H-16 dihedral angle values for the four simulated diastereoisomers of belizeanic acid.

the C-14→C-24 fragment, all of which derive from acetate oxygen.

According to the biosynthetic origin of the carbon atoms determined by our group and their own results about the origin of the oxygen atoms,[27] Murata et al. proposed the bioconstruction of the C-16→C-26 ring system of OA from a polyene precursor. This would give a β-epoxide intermediate through atmospheric oxidation and subsequently, a nucleophilic cyclisation initiated by the attack of the hydroxyl group at C-25 would give the polyheterocyclic system present in OA (Scheme 1). Therefore, the identification of BA is crucial to reinforce the previous hypotheses. Considering that the fragment C-11→C-24 (in which the differences between AO and BA are located) clearly seems to be a classic polyketide formed by the consecutive condensation of seven acetate units catalyzed by polyketide synthetases (PKS) in a similar manner to that demonstrated for the structurally related polyether monensin,[28] we think that the elongation of the C-17→C-18 acetate unit in the precursor polyene should be different for OA and BA. Thus, although for OA the PKS module of enzymes involved in this step would consist of a ketosynthetase (KS) and an acyl-transferase (AT), for BA the same module must also include an active ketoreductase (KR). As a result, slightly different precursors for each molecule would be synthesised, the reduction of the C-19 carbonyl group in OA to a hydroxyl group in BA being the difference between them. Precisely the absence of such a carbonyl group would lead to the formation of just one oxane ring in BA (corresponding to the E ring in OA) and precludes the formation of the C, D and E ring systems present in OA (Scheme 1).

We believe that enough bibliographic data is currently available to support the above hypothesis. Although no gene homologous with other domains in known type I PKS has been reported in dinoflagellates, the gene products deduced in *Amphidinium sp.*[29] showed similarities to them, and PKS-encoding genes have been localised in *Karenia sp.*, though not yet linked to toxin production.[30,31] Moreover, studies of the protist *Cryptosporidium parvum*, considered the organism most closely related to dinoflagellates that is known to encode type I PKS, allowed identification of the gene encoding several enzymatic domains within this protein.[32,33] The protein is organised into a loading domain that consists of an acyl-CoA ligase and an acyl carrier protein (ACP), seven elongation modules containing between two and five of the six domains required for the elongation of C_2 acyl units (KS, ketosynthetase; AT, acyl transferase; DH, dehydratase, ER, enoylreductase, KR, ketoreductase and/or ACP) and a carboxy end homologous to various reductases. In addition, it is also known that ER, DH and/or KR may be inactive or dysfunctional in some modules due to a partial deletion or incorrect consensus amino acid sequence,[34–36] so the activation of an inactive KR would give the reduced polyene precursor necessary to obtain BA.

One important feature of the above biosynthetic hypothesis is the stereochemistry of BA, which must be identical to that of OA at C-23, C-24 and C26, as observed. However,

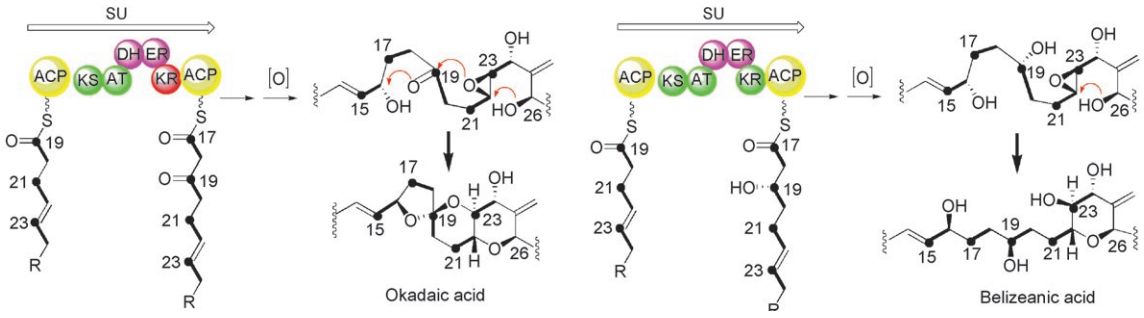

Scheme 1. Biosynthetic proposal for the fragment C-16→C-24 of okadaic acid (OA) and belizeanic acid (BZ). SU, synthetic unit or module; ACP, acyl carrier protein; KS, ketosynthetase; AT, acyl transferase; DH, dehydratase; ER, enoylreductase; KR, ketoreductase. Functional enzymes are represented in yellow and green; inactive in red and nonfunctional in purple. Bold lines correspond to acetate unit.

according to our proposal, the stereochemistry of the polyene precursor at C-16 should be *S* as the inversion of its chirality by means of the nucleophilic attack of the hydroxy group at C-19 would give the observed chirality 16*R* in OA. In fact, the 16*S** stereochemistry is what we propose for BA according to our conformational studies. Nothing can be said, however, about the stereochemistry of the key C-19 position according to our hypothesis.

Biological activity: The biological activity of BA was assessed by using one of the main targets of OA, the serine/threonine protein phosphatase type 1 (Figure 7).[37] OA is the archetypical inhibitor of this enzyme and was, therefore, used as a control.[38] Despite the opening of two rings, BA still turned out to be a potent inhibitor. The inhibitory activity of the toxin versus PP 1 showed a slight loss of activity relative to OA. In vitro assays showed that BA presents an IC_{50} of 318 ± 37 nM, whereas OA showed an IC_{50} of 62 ± 6 nM.

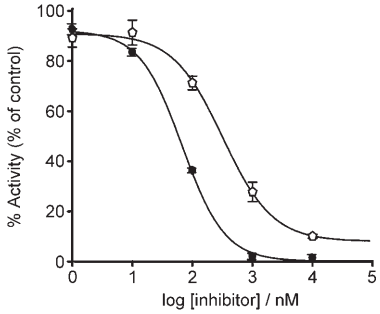

Figure 7. Inhibitory effects of belizeanic acid (BA, pentagon) and okadaic acid (OA, circle) on PP1. Each symbol represents the average of five measurements. Vertical bars indicate standard errors of means.

Docking: A computational study consisting of molecular docking calculations was undertaken to investigate the possible interaction mode of BA within the PP1 binding site. The Ser/Thr phosphatases are metal-dependent enzymes, thus the presence of two Mn^{2+} ions in the active site of PP1, which could directly coordinate a number of water molecules, complicated the use of this protein as a docking model, because any of the water molecules, or even the metal atoms, could potentially be displaced upon inhibitor binding.[39] After examination of the crystal structures of PP1 in complex with OA,[40] microcystin LR,[41] motuporin[42] and calyculin A,[43] we decided to perform calculations with both metal ions and one water molecule directly coordinated, as present in those complexes.

First of all, preliminary calculations were made to optimise the running parameters to be used with the Autodock software[44] and to verify that in our hands the software could be used to dock a similar inhibitor within the PP1 binding site. For this purpose, the crystallographic complex between PP1 and OA (pdb code: 1JK7) was used as a control structure. As a result of the previous calculations, a single cluster containing all conformers in the correct orientation inside the binding site was obtained. In fact, a root-mean-square deviation (RMSD) of 1.05 Å (calculated on the heavy atoms) with respect to the position observed in the crystal structure was obtained. The ability to accurately predict the bound conformation of OA suggests that Autodock would show similar accuracy with the same kind of compounds docked into the PP1 binding site. Once a reliable docking protocol was established, we decided to use it to dock BA into the crystallographic structure of PP1. First, the coordinates of PP1 in complex with OA as deposited at the Protein Data Bank were refined by using a molecular-mechanics minimisation using the OPLS-AA force field.[45] Then, the BA structure was docked into the PP1 binding site. Finally, the resulting complexes were further minimised with Macromodel using a GBSA continuum solvation model.

The docking results suggested that BA fits into the binding site adopting a pseudocyclic conformation, resembling experimental observations for OA. Moreover, the proposed structure also shows an intramolecular hydrogen bond between the C-27-OH and the carbonyl at C-1 (Figure 8) However, the orientation of BA in the active site of PP1 (characterised by the presence of three adjacent grooves: C-terminal, acidic and hydrophobic)[41] shows an important difference to that shown by OA. Surprisingly, the C-30→C-38 spiroketal moiety of BA fits into the acidic groove instead of into the hydrophobic groove, as observed for OA. However, calyculin A, another potent PP1 inhibitor, fills the acidic groove in a very similar way to what we found for BA, thus supporting our proposal (Figure 9).[43] Moreover, there is still a comparable number of protein–ligand hydrophobic contacts if we compare the crystallographic structure

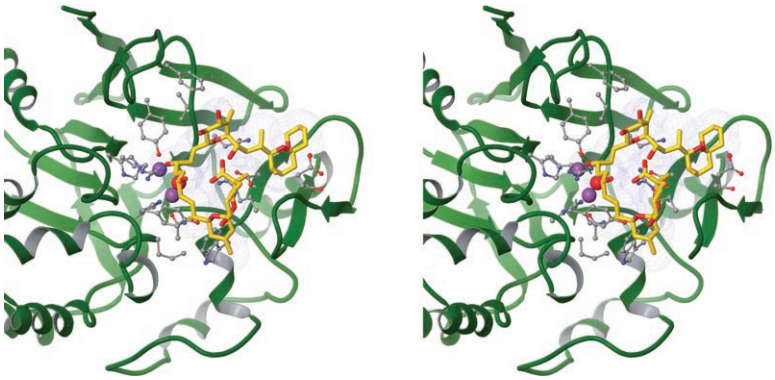

Figure 8. Stereoview of the PP1 active site in complex with the docked structure of belizeanic acid. Only those residues within a distance of 3 Å of the inhibitor are shown. Purple and red spheres represent Mn^{2+} and water, respectively.

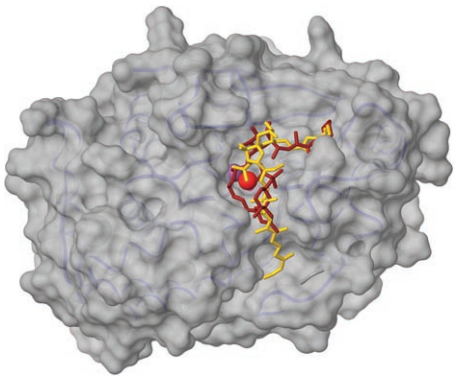

Figure 9. Superposition of the crystallographic structure of the PP1–calyculin A complex (yellow) and the best-energy docked structure of belizeanic acid (red). Purple and red spheres represent Mn^{2+} and water, respectively.

of PP1–OA and the docked structure of BA in this protein (Figure 10). Residues Trp-206 and Ile-130 of PP1 are still involved in important hydrophobic interactions, but now with the C-4→C-15 region of BA instead of the C-19→C-38 region of OA. Val-250 is also involved in these kinds of interactions with the C-20→C-28 region of BA, however, the Phe-276 residue is now further away from the ligand, releasing some of the strain caused in the OA complex. Following

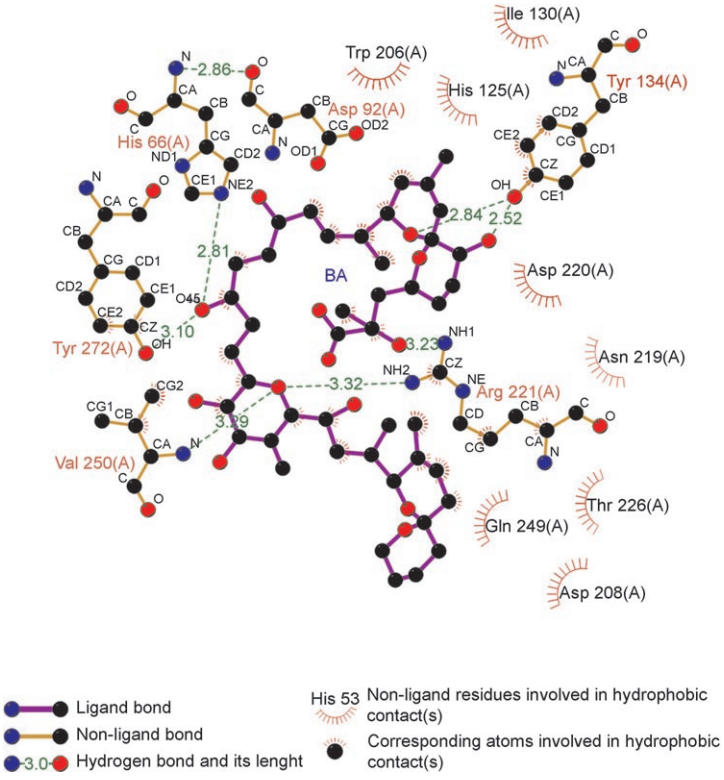

Figure 10. 2D cartoon produced by the program ligplot showing those PP1 residues interacting with belizeanic acid. Hydrophobic contacts and distances of all possible intermolecular hydrogen-bonding interactions are shown.[46]

the characteristic pattern of the OA class of toxins, the carboxylic acid region of the inhibitor is filling the metal binding site of the protein, the hydroxyl group at C-19 being the only group within 3 Å of the metals: by using the best-energy docked conformer, it was located a distance of 2.2 Å from one of the manganese ions and 2.6 Å from the conserved water molecule. Regarding the possible hydrogen-bond interactions, these could occur between Tyr-134 and the C-7 hydroxyl and the ether-oxygen C-8/C-12, as well as between both Tyr-272 and His-66 and the C-19 hydroxyl group of BA. The crucial hydrogen-bond interaction observed between Arg-221 and the hydroxyl at C-24 in OA is substituted in BA by those between the hydroxyl at C-2 and the ether-oxygen at C-22/C-26. The same docking calculations were undertaken for the other three possible diastereoisomers. The results were very similar to those commented for the 16*S**19*S** isomer (see Supporting Information).

Conclusion

A new protein phosphatase 1 inhibitor, belizeanic acid, was isolated from cultures of the dinoflagellate *P. belizeanum*. This compound maintains those elements that have been identified as key for PP inhibitors, that is, the carboxyl and the hydroxyl groups at C-1 and C-2 as well as the hydroxyl at C-24 and the hydrophobic moiety C-30–C-38, though it shows rings C and D open, a unique structural feature among OA derivatives. It could be regarded as a structural simplification of the OA skeleton that could be used to synthesise new phosphatase inhibitors more easily. Results of NMR analysis and molecular-mechanics calculations indicate that although BA is a highly flexible molecule, it shows a preferred conformation in solution. This fact led us to determine the relative stereochemistries of carbons C-16 and C-19 as *S** for both chiral centres. At the same time, the isolation of this metabolite supports the hypothesis of Murata et al. concerning the biosynthetic origin of the C-16→C-26 ring system of OA from a polyene precursor, through intermediate atmospheric oxidation and subsequent nucleophilic cyclisation. According to this mechanism, the expected stereochemistry of BA matches that determined by us. We also propose a model of the binding mode of BA to the catalytic subunit of protein phosphatase 1, in which BA fills the catalytic site and the acidic groove of the enzyme. This result is different to what might be predicted from a simple and direct extrapolation of the structure of the PP1–OA complex, but it agrees well with the results found for the more flexible ligand calyculin A when it is bound to the same protein.

In summary, we believe that this study should be significant for the design of new PP1 inhibitors with simpler structures and improved activities.

Experimental Section

General experimental procedures: Mass spectra were recorded on a VG AutoSpec FISON spectrometer. Optical rotation was determined on a Perkin–Elmer 241 polarimeter using a sodium lamp operating at 589 nm. The IR spectrum was measured on a Bruker IFS55 spectrometer. HPLC was carried out with an LKB 2248 system equipped with a photodiode array detector. TLC was performed on AL Si gel Merck 60 F_{254} and TLC plates were visualized by spraying with phosphomolybdic acid reagent and heating.

NMR experiments: NMR spectra were recorded at 298 K on a Bruker Avance 400 spectrometer. The compound was dissolved in 250 μL of CD_3OD in a Shigemi tube. COSY, 1D/2D TOCSY, HSQC, HMBC and ROESY experiments were performed using standard pulse sequences. ^1H–^{13}C HMBC were optimised for $^1J_{C,H}=135$ Hz and $^{2,3}J_{C,H}=10$ Hz, respectively. Phase-sensitive ROESY spectra were measured using a mixing time of 400 ms as the intensity of the NOESY cross peaks were close to zero at RT. The volume integrals of the individually assigned ROE cross peaks were converted into distance constrains using the isolated spin-pair approximation, taking into account the offset effect. $^3J_{H,H}$ values were measured from 1D ^1H NMR, or when signals overlapped, from the TOCSY. Data were processed using MestRec software.

Belizeanic acid: Amorphous solid; $[\alpha]_D=+2.74$ ($c=0.073$ in MeOH); ^1H NMR (400 MHz, [D$_4$]MeOH, 25 °C): $\delta=5.74$ (dd, $J_{13,14}=8.5$, $J_{14,15}=15.5$ Hz, 1H; H-14), 5.44 (dd, $J_{14,15}=5.5$, $J_{15,16}=6.6$ Hz, 1H; H-15), 5.18 (s, 1H; H-9), 5.18 (s, 1H; H-41), 4.92 (s, 1H; H-41′), 3.98 (m, 1H; H-27), 3.97 (m, 1H; H-4), 3.97 (m, 1H; H-16), 3.93 (m, 1H; H-24), 3.82 (d, $J_{26,27}=8.8$ Hz, 1H; H-26), 3.72 (m, $J_{12,13}=7.1$ Hz, 1H; H-12), 3.63 (m, 1H; H-38), 3.57 (m, 1H; H-19), 3.55 (m, 1H; H-22), 3.44 (m, 1H; H-38′), 3.27 (m, 1H; H-7), 3.18 (dd, $J_{29,30}=9.8$ Hz, 1H; H-30), 2.91 (t, $J=9.19$ Hz, 1H; H-23), 2.26 (m, 1H; H-13), 2.08 (m, 2H; H-20), 1.96 (m, 1H; H-32), 1.91 (m, 1H; H-11), 1.83 (m, 1H; H-6), 1.82 (m, 1H; H-3), 1.82 (m, 1H; H-29), 1.81 (m, 1H; H-36), 1.74 (m, 1H; H-31), 1.73 (m, 1H; H-11′), 1.70 (m, 1H; H-5), 1.65 (m, 2H; H-17), 1.65 (s, 3H; H-43), 1.60 (m, 1H; H-3′), 1.60 (m, 2H; H-17), 1.59 (m, 1H; H-6′), 1.54 (m, 1H; H-35), 1.52 (m, 2H; H-18), 1.44 (m, 1H; H-36′), 1.44 (m, 2H; H-37), 1.33 (m, 1H; H-35′), 1.29 (m, 1H; H-28), 1.28 (m, 1H; H-32′), 1.27 (m, 2H; H-33), 1.20 (m, 1H; H-5′), 1.20 (m, 3H; H-44), 1.03 (d, $J_{13,42}=7.0$ Hz, 3H; H-42), 0.97 (d, $J_{29,40}=6.32$ Hz, 3H; H-40), 0.85 (m, 1H; H-28′), 0.85 ppm (d, $J_{31,39}=6.87$ Hz, 3H; H-39); ^{13}C NMR (100 MHz, [D$_4$]MeOH, 25 °C): $\delta=$ 182.5, 146.4, 139.3, 134.5, 133.9, 123.2, 110.6, 97.6, 96.2, 85.1, 78.1, 76.6, 76.3, 74.0, 73.8, 72.8, 71.9, 71.6, 70.7, 68.0, 65.6, 60.8, 46.2, 42.2, 36.4, 36.4, 33.6, 32.7, 31.8, 31.7, 31.1, 30.8, 30.1, 28.3, 27.8, 27.6, 27.4, 27.3, 25.9, 22.5, 19.2, 16.7, 16.2, 10.7 ppm; IR (KBr): $\tilde{\nu}_{max}=3393$, 2927, 2857, 1732, 1601, 1458, 1385, 1238, 1180, 1088 cm^{-1}; MS-ES: m/z: calcd for $[C_{44}H_{72}O_{14}+Na]^+$: 847.4820; found: 847.7.

Cell cultures: A sample of 3 mL of a clonal culture of the dinoflagellate *P. belizeanum* containing approximately 7000 cells per ml was obtained from the IEO de Vigo collection by courtesy of Santiago Fraga. This sample was upscaled to perform large-scale cultures in 80-L tanks containing 40-L tanks of sea water enriched with Guillard K medium up to a final volume of 1020 L. Cultures were incubated statically at 23 °C using 16:8 light/dark cycles for three weeks.

Extraction and isolation: Due to the benthonic nature of the dinoflagellate *Prorocentrum belizeanum*, most of the supernatant was easily separated and the cells were harvested by centrifugation at $3000\times g$. The cells were then sonicated and extracted with acetone (4×1 L), and the resulting extract was filtered and concentrated to obtain 22.1 g of crude extract. The extract was subjected to successive chromatography procedures: first, a gel filtration step was performed using Sephadex LH-20 (Ø = 6.5 cm × 60 cm) with a mixture of $CHCl_3$/MeOH/*n*-hexane (1:1:2) to yield three fractions. The second fraction (8.11 g) was further fractionated using medium-pressure reversed-phase LOBAR B (Ø = 25 mm × 310 mm) LiChroprep columns eluted with MeOH/H_2O 17:3. Finally, active fractions were subjected to HPLC purification on an XTerra (Ø = 1.9 cm × 15 cm) column eluted with CH_3CN/H_2O 1:1. A final yield of 0.5 mg of belizeanic acid was obtained.

Biological assays: PP1c was purchased from New England Biolabs. Protein phosphatase activity was assayed at 37 °C using 0.050 units μL^{-1} of protein and 100 μM of fluorescein diphosphate as substrate, essentially by the method described previously.[38] The reaction was monitored by fluorescence spectroscopy at 485–535 nM. Data were fitted to a one-site binding model. Assays with belizeanic acid were performed in quintuplicate ($n=5$), but for okadaic acid only duplicates ($n=2$) were used.

Conformational searches and dynamics of belizeanic acid: Calculations were performed using the MacroModel 8.5 software and the MMFF94s force field. Solvation effects were simulated using the generalised Born/surface area (GBSA) water-solvent model. Extended nonbonded cutoff distances (a van der Waals cutoff of 8.0 Å and an electrostatic cutoff of 20.0 Å) were used. The crystal structure of OA was used as a template to build the structure of BA by removal of the appropriate covalent bonds.[16] The chirality of C-16 and C-19 was then adapted to build four possible diastereoisomers of BA (16*S*19*S*, 16*S*19*R*, 16*R*19*S*, 16*R*19*R*) and the resulting structures were used as the starting point for the conformational searches. Four different random-seeded conformational searches (one for each diasteroisomers) were undertaken using 100000 Monte Carlo multiple minimum steps and the TNCG algorithm. All local minima within 50 kJ of the global minimum were saved and subsequently re-minimised using the FMNR algorithm and an energy cutoff of 25 kJ. Duplicate conformations (0.25 Å rmsd) were removed. This procedure generated 486, 319, 1032 and 652 structures for the 16*S*19*S*, 16*S*19*R*, 16*R*19*S*, 16*R*19*R* diasteroisomers, respectively. Next, a search within each conformer pool was performed to select only those structures showing dihedral angles within a range of 180 ± 40° for the C26-C30 moiety. The selected conformers from each run (one for each diasteroisomer) were then combined and their stereochemistry adapted to become 16*S*19*S*, 16*S*19*R*, 16*R*19*S* and 16*R*19*R*. Next, the resulting conformers were fully optimised to convergence using the FMNR algorithm and a 25-kJ mol^{-1} energy cutoff. Finally, XCluster[22] was used to group conformations with similar dihedral angles. The number of structures was finally reduced to 48, 37, 51 and 54 for the 16*S*19*S*, 16*S*19*R*, 16*R*19*S*, 16*R*19*R* diasteroisomers, respectively. All molecular dynamics simulations were performed using the same general conditions used for the MCMM searches. Four MD simulations of 4 ns each (one for each diasteroisomer) were run at 300 K using the SHAKE algorithm. A time step of 1.5 fs was used.

Docking: The AutoDock 3.0.5 and 4.0 software packages as implemented through the graphical user interface AutoDockTools (ADT) 1.4.6, were used to dock OA and BA to the catalytic subunit of PP1.[44] The reliability of the docking protocol was first tested by simulations of the binding mode of okadaic acid followed by comparison of the modeled complex with the corresponding crystallographic structure (pdb code: 1JK7). The program successfully reproduced the OA bound conformation (rmsd of 0.005 A) as well as its X-ray coordinates relative to the binding site (rmsd of 1.05 A). For docking, the enzyme file was prepared using the coordinates of the PP1-OA complex (1JK7) in which the ligand was removed and a structure optimisation was performed using the OPLS-AA force field and the Polak–Ribiere conjugate–gradient method. A continuum solvation method (GB/SA) using water as the solvent was utilised. The optimised structure was used to perform docking calculations with the BA structure. The two metal atoms and one coordinating water molecule were retained with the protein structure. The metal atoms were each manually assigned a charge of +2 and a solvation value of −30. All other atoms were generated automatically by ADT. The docking area was set around the active site. Grid maps of 60 Å × 60 Å × 60 Å with 0.375-Å spacing were calculated for each atom probe (characterised by the same stereoelectronic properties as the atoms constituting the inhibitor) using AutoGrid. The Lamarckian genetic algorithm (LGA) method was selected to generate the orientations/conformations of the ligand within the active site. First, 250 Lamarckian genetic algorithm local search (GALS) runs were performed with a population of 50 individuals, an energy evaluation number of 50×10^6 and 300 rounds of Solis and Wets local search with a probability of 0.06, using AutoDock 3.0.5. The first ranked conformation was used as input for subsequent searches using AutoDock 4.0, setting the software to use that conformation. This time, 200 GALS runs using a population of 200 individuals and maximum of 50×10^6 energy evaluations were performed. The docking results were clustered on the

basis rmsd between the coordinates of the atoms (using a 1.5-Å cluster tolerance) and ranked on the basis of free energy of binding.

Acknowledgements

This research was funded by Grants AGL2005-07924-C04—01 from the Ministry of Education and Science of Spain and by the EU project VALBIOMAR. P.G.C. acknowledges ICIC for a predoctoral grant.

[1] T. Yasumoto, M. Murata, Y. Oshima, M. Sano, G. K. Matsumoto, J. Clardy, *Tetrahedron* **1985**, *41*, 1019–1025.
[2] A. H. Daranas, M. Norte, J. J. Fernandez, *Toxicon* **2001**, *39*, 1101–1132.
[3] M. Suganuma, H. Fujiki, H. Suguri, S. Yoshizawa, M. Hirota, M. Nakayasu, M. Ojiva, K. Wakamatsu, K. Yamada, T. Sugimura, *Proc. Natl. Acad. Sci. USA* **1988**, *85*, 1768–1771.
[4] P. Anderson, H. Enevoldensen, D. Anderson in *Manual of Harmful Marine Microalgae: Monographs on Oceanographic Methodology* (Eds.: G. M. Hallegraeff, D. M. Anderson, A. D. Cembella), UNESCO, Paris, **2003**, pp. 627–647.
[5] C. Biolojan, A. Takai, *Biochem. J.* **1988**, *256*, 283–290.
[6] D. A. Colby, A. R. Chamberlin, *Mini-Rev. Med. Chem.* **2006**, *6*, 657–665.
[7] A. H. Daranas, P. G. Cruz, A. H. Creus, M. Norte, J. J. Fernandez, *Org. Lett.* **2007**, *9*, 4191–4194.
[8] J. J. Fernandez, M. L. Candenas, M. L. Souto, M. M. Trujillo, M. Norte, *Curr. Med. Chem.* **2002**, *9*, 229–262.
[9] M. Isobe, Y. Ichikawa, T. Goto, *Tetrahedron Lett.* **1986**, *27*, 963–966.
[10] C. J. Forsyth, S. F. Sabes, R. A. Urbanek, *J. Am. Chem. Soc.* **1997**, *119*, 8381–8382.
[11] S. V. Ley, A. C. Humphries, H. Eick, R. Downhan, A. R. Ross, R. J. Boyce, J. B. J. Pavey, J. Pietruszka, *J. Chem. Soc. Perkin Trans. 1* **1998**, 3907–3912.
[12] M. Norte, R. Gonzalez, J. J. Fernandez, M. Rico, *Tetrahedron* **1991**, *47*, 7437–7446.
[13] M. Falk, P. F. Spierenburg, J. A. Walter, *J. Comput. Chem.* **1996**, *17*, 409–417.
[14] M. Gavagnin, M. Carbone, P. Amodeo, E. Mollo, R. M. Vitale, V. Roussis, G. Cimino, *J. Org. Chem.* **2007**, *72*, 5625–5630.
[15] H. Gouda, T. Sunazuka, H. Ui, M. Handa, Y. Sakoh, Y. Iwai, S. Hirono, S. Omura, *Proc. Natl. Acad. Sci. USA* **2005**, *102*, 16286–16291.
[16] K. Tachibana, P. J. Scheuer, Y. Tsukitani, H. Kikuchi, D. Van Engen, J. Clardy, Y. Gopichand, F. J. Schmitz, *J. Am. Chem. Soc.* **1981**, *103*, 2469–2471.
[17] P. G. Cruz, A. H. Daranas, J. J. Fernandez, M. Norte, *Org. Lett.* **2007**, *9*, 3045–3048.
[18] A. H. Daranas, J. J. Fernandez, E. Q. Morales, M. Norte, J. A. Gavin, *J. Med. Chem.* **2004**, *47*, 10–13.
[19] T. A. Halgren, *J. Comput. Chem.* **1996**, *17*, 490–519.
[20] F. Mohamadi, N. G. J. Richards, W. C. Guida, R. Liskamp, M. Lipton, C. Caufield, G. Chang, T. Hendrickson, W. C. Still, *J. Comput. Chem.* **1990**, *11*, 440–467.
[21] W. C. Still, A. Tempczyk, R. C. Hawley, T. Hendrickson, *J. Am. Chem. Soc.* **1990**, *112*, 6127–6129.
[22] P. S. Shenkin, D. Q. McDonald, *J. Comput. Chem.* **1994**, *15*, 899–916.
[23] M. Norte, A. Padilla, J. J. Fernandez, *Tetrahedron Lett.* **1994**, *35*, 1441–1444.
[24] J. L. C. Wright, T. Hu, J. L. McLachlan, J. Neeham, J. A. Walter, *J. Am. Chem. Soc.* **1996**, *118*, 8757–8758.
[25] A. H. Daranas, J. J. Fernandez, M. Norte, J. A. Gavin, B. Suarez-Gomez, M. L. Souto, *Chem. Rec.* **2004**, *4*, 1–9.
[26] M. Murata, M. Izumikawa, K. Tachibana, T. Fujita, H. Naoki, *J. Am. Chem. Soc.* **1998**, *120*, 147–151.
[27] M. Izumikawa, M. Murata, K. Tachibana, T. Fujita, H. Naoki, *Eur. J. Biochem.* **2000**, *267*, 5179–5183.
[28] A. R. Gallimore, C. B. W. Strak, A. Bahtt, B. M. Harvey, Y. Demydchuk, V. Bolaños-García, D. J. Fowler, J. Staunton, P. F. Leadlay, J. B. Spencer, *Chem. Biol.* **2006**, *13*, 453–460.
[29] T. Kubota, Y. Iinuma, J. Kobashi, *Biol. Pharm. Bull.* **2006**, *7*, 1314–1318.
[30] R. V. Snyder, P. D. L. Gibbs, A. Palacios, L. Abiy, R. Dickey, J. V. Lopez, K. S. Rein, *Mar. Biotechnol.* 2003, 5, 1–12.
[31] R. V. Snyder, M. A. Guerrero, C. D. Sinigalliano, J. Winshell, R. Perez, J. V. Lopwz, K. S. Rein, *Phytochemisty* **2005**, *66*, 1767–1780.
[32] G. Zhu, M. J. Marchewka, K. M. Woods, S. J. Upton, J. S. Keithly, *Mol. Biochem. Parasitol.* **2000**, *15*, 253–260.
[33] G. Zhu, M. J. LaGier, F. Stejskal, J. J. Millership, X. Cai, J. S. Keithly, *Gene* **2002**, *298*, 79–89.
[34] H. Ikeda, S. Omura, *Chem. Rev.* **1997**, *97*, 2591–2609.
[35] B. Shen, *Curr. Opin. Chem. Biol.* **2003**, *7*, 285–295.
[36] E. Rodriguez, R. McDaniel, *Curr. Opin. Microbiol.* **2001**, *4*, 526–534.
[37] A. McCluskey, T. R. Sim, J. A. Sakoff, *J. Med. Chem.* **2002**, *45*, 1151–1175.
[38] J. M. Vieytes, O. I. Fontal, F. Leira, J. M. V. Baptista de Sousa, L. M. Botana, *Anal. Biochem.* **1997**, *248*, 258–264.
[39] J. P. Rogers, A. E. Beuscher, M. Flajolet, T. McAvoy, A. C. Nairn, A. J. Olson, P. Greengard, *J. Med. Chem.* **2006**, *49*, 1658–1667.
[40] J. T. Maynes, K. S. Bateman, M. M. Cherney, A. K. Das, H. A. Luu, C. F. Holmes, M. N. James, *J. Biol. Chem.* **2001**, *276*, 44078–44088.
[41] J. Goldberg, H. Huang, Y. Kwon, P. Greengard, A. C. Nairn, J. Kuriyan, *Nature* **1995**, *376*, 745–753.
[42] J. T. Maynes, H. A. Luu, M. M. Cherney, R. J. Andersen, D. Williams, C. F. Holmes, M. N. James, *J. Mol. Biol.* **2006**, *356*, 111–120.
[43] A. Kita, S. Matsunaga, A. Takai, H. Kataiwa, T. Wakimoto, N. Fusetani, M. Isobe, K. Miki, *Structure* **2002**, *10*, 715–724.
[44] G. M. Morris, D. S. Goodsell, R. S. Halliday, R. Huey, W. E. Hart, R. K. Belew, A. J. Olson, *J. Comput. Chem.* **1998**, *19*, 1639–1662.
[45] W. L. Jorgensen, D. S. Maxwell, J. Tirado-Rives, *J. Am. Chem. Soc.* **1996**, *118*, 11225–11235.
[46] A. C. Wallace, R. A. Laskowski J. M. Thornton, *Prot. Eng.* **1995**, *8*, 127–134.

Received: March 31, 2008
Published online: July 4, 2008

